International Journal of Scientific Engineering and Science
Volume 8, Issue 12, pp. 40-53, 2024. ISSN (Online): 2456-7361

Advanced Multi-Level Control for Efficient Energy Management in Microgrids

Edrees Yahya Alhawsawi[1], Mohamed A. Zohdy[1], Ahmed M. Annekaa[2]
[1]Department of Electrical and Computer Engineering, Oakland University, Rochester, MI 48309, USA
[2]Department of Electrical and Computer Engineering, College of Electronic Technology, Tripoli 20299, Libya.
*Corresponding author: ealhawsawi@oakland.edu

***Abstract*—** *This paper proposes a multi-level control strategy for hybrid microgrid management, integrating renewable energy sources such as solar and wind with conventional systems like Combined Heat and Power (CHP) units, Battery Energy Storage Systems (BESS), and grid electricity. The Oakland University campus served as a case study to evaluate the effectiveness of Adaptive Model Predictive Control (AMPC) in optimizing energy distribution, mitigating fluctuations in renewable generation, and minimizing grid dependency. The AMPC system dynamically responded to real-time conditions, efficiently charging BESS during periods of surplus generation and ensuring seamless operation during peak demand. When compared to basic MPC, AMPC exhibited enhanced performance in meeting load requirements, improving renewable energy utilization, and achieving significant cost reductions, particularly during seasonal extremes. This scalable and adaptable framework illustrates the potential of AMPC for future microgrid systems, offering a sustainable, cost-effective solution as renewable technologies continue to advance.*

***Keywords*—** *Multilevel-control Renewablw energy, Microgrid, Adaptive MPC, Energy Management.*

I. INTRODUCTION

Adopting a utility power source is an ineffective solution due to its dependence on fossil fuels, which are both costly and harmful to the environment. Therefore, transitioning to renewable energy sources (RESs) is essential due to their substantial benefits [1]. RESs, including wind, solar, geothermal systems, biomass, tidal, and hydroelectricity, are more effective, reliable, and require minimal maintenance, while efficiently reducing carbon dioxide (CO_2) emissions and creating a quieter environment [2-5]. A microgrid is a self-sustaining power system capable of operating both in connection with the main power grid and independently, supplying electricity to facilities like university campuses, commercial buildings, and hospital complexes [6]. Microgrids have become vital solutions for decentralized and independent power systems in light of the growing need for energy security, reliability, and environmental sustainability [7]. In these systems, Distributed Energy Resources (DERs) are integrated, including renewable energy sources such as Photovoltaic (PV) systems and Wind Turbines (WT), conventional energy sources like Combined Heat and Power (CHP) units, Energy Storage Systems (ESS), and a variety of load demands[8]. University campuses, with their complex and ever-changing load requirements, have become ideal targets for microgrid implementation, both for actual application and as research objects [6]. There are many benefits associated with microgrids; for instance, they are able to operate autonomously, hence providing more reliability when compared with the traditional centralized power system [9]. Secondly, microgrids can also integrate faster renewable energy and reduce dependency on the fossil fuels [10], and have increased flexibility and control due to their decentralized nature [11]. However, using renewable and conventional energy is a problem since renewable energy sources are often intermittent and require efficient energy management. To manage these challenges, it is necessary to have effective control strategies focused on the reduction of energy utilization which can be challenging in a campus setting where demand is not always steady, and where it is important to integrate several sources of energy.

This is the reason microgrid controllers are involved in managing these complexities as they control the interconnection between DERs, ESSs, as well as loads and the grid. Hierarchical control strategies refer to the division of control tasks in the microgrid by the primary, secondary, and tertiary levels, which have been identified as efficient methods of coping with the complexities of energy systems in the microgrid. These strategies facilitate optimal utilization of the microgrid since the communication and control between the microgrid's components is continuously adaptive to the prevailing situation. Given the complex energy demands of a university campus encompassing research facilities, classrooms, dormitories, and recreational centers microgrid controllers must be sophisticated to ensure dependability, stability, and efficiency [12]. These controllers are designed to operate in grid-connected mode and manage multiple Distributed Energy Resources (DERs) and Energy Storage Systems (ESSs), enabling efficient energy usage while ensuring continued operations during power outages. According to the authors in [8], this property helps to maintain the continuity of the electricity supply in the event of a power failure.

The objective of this research is to optimize energy management in a hybrid microgrid at Oakland University by implementing Adaptive Model Predictive Control (AMPC) within a multi-level control framework. This approach, a modified version of traditional MPC with dynamic prediction horizons, enhances energy efficiency and reduces reliance on the utility grid by adjusting power flows between solar photovoltaic (PV) panels, wind turbines (WT), combined heat and power (CHP) units, and energy storage systems (ESS). By leveraging local solar and wind resources, the system ensures real-time adaptation to fluctuations, improves operational sensitivity, reduces costs, and maintains stability in complex environments.

International Journal of Scientific Engineering and Science
Volume 8, Issue 12, pp. 40-53, 2024. ISSN (Online): 2456-7361

Section two provides an overview of microgrid working principles and summarizes existing literature on control systems. Section three outlines the proposed methodology, while section four presents the simulation results and discussions. Finally, the paper concludes in section five.

II. MICROGRID CONTROL SYSTEM

Model Predictive Control (MPC) is an advanced control technique that optimizes the next control action by predicting future behavior over a defined horizon while adhering to system constraints. It ensures the system output follows a desired reference trajectory, even in the presence of constraints on inputs and states. MPC is particularly effective for nonlinear systems, as it can linearize the model at each state, apply optimization, and adjust as needed. Its flexibility in adjusting control actions makes MPC superior to traditional controllers for maintaining system stability and performance. Due to its strong performance, MPC has been widely applied across various processes and industries, including renewable energy systems [13-15], automotive applications [16-19], and manufacturing sectors [20-22]. Figure 1 shows the general concept of MPC.

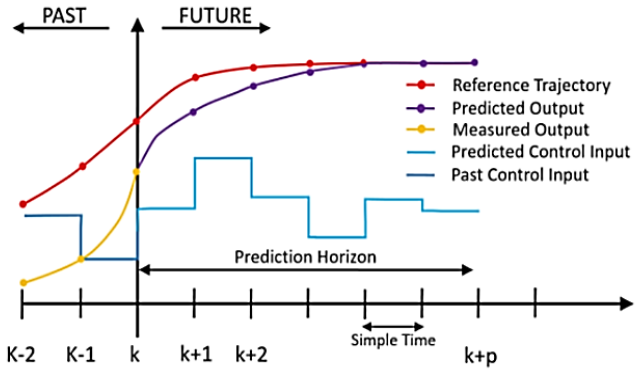

Figure. 1 The General Concept of MPC [23]

The design of an MPC relies on the discrete state-space matrices of the system model, represented as A_d, B_d, and C_d, along with key parameters like the control horizon (NC) and prediction horizon (NP). NP defines the number of future samples used for making predictions, while the control horizon NC indicates the number of samples used to adjust the system's output. These parameters are selected according to the rule: $1 \leq NC \leq NP$. Given the advantages and robust performance of MPC, it is well-suited for optimizing output power of renewable energy.

i. Prediction

The output of the future system model is predicted using estimated control input vectors and future state variables over the prediction horizon (N_P). Consequently, the future control input trajectory and future state variables can be represented by the follow equations:

$$u(k),\ u(k+1), u(k+2),\ \ldots, u(k+N_C-1) \quad (1)$$

$$x(k+1|k), x(k+2|k), \ldots, x(k+N_P|k) \quad (2)$$

Where: $u(k)$ and $x(k)$ represent the input control variable and state vector at time (k), respectively. By iteratively implementing the equations for the input control and state vector, the predicted sequence of the output Y is generated, as shown below.

$$Y = Fx(k_i) + \emptyset\, U \quad (3)$$

Where: F and $\emptyset$ are matrices used in the prediction Equation (4)

$$F = \begin{bmatrix} CA \\ CA^2 \\ \vdots \\ CA^{N_p} \end{bmatrix} \quad \emptyset = \begin{bmatrix} CB & 0 & & 0 \\ CAB & CB & & 0 \\ CA^2B & CAB & \cdots & 0 \\ \vdots & \vdots & & \vdots \\ CA^{N_P-1}B & CA^{N_P-2}B & & CA^{N_P-N_C}B \end{bmatrix} \quad (4)$$

ii. Optimization

The objective of the control design is to ensure that the predicted power $P(k)$ of the renewable energy system tracks the predefined reference signal $r\,(k_i)$ by determining the optimal control vector u to minimize the prediction error over the horizon N_P. The predefined reference signal is defined below.

$$r(k) = [r(k+1) \quad r(k+2) \quad r(k+3) \quad \ldots \quad r(k+N_P)]^T \quad (5)$$

The cost function:

$$J(k) = \sum_{i=1}^{N_p} Q.[(\hat{T}(k+i|k) - r(k+i|k)]^2 + \sum_{i=1}^{N_C-1} R.[\Delta v(k+i|k)]^2 + \sum_{i=1}^{N_P} Q_1.[v(k+i|k)]^2 \quad (6)$$

Subjected to:

$$P_{min} \leq \hat{P}(k+i|k) \leq P_{max} \quad (7)$$

Where: $(\hat{T}(k+i|k)$ and $r(k+i|k)$ represent the predicted output power and predefined reference power at time $(k+i)$ respectively. Additionally, $v(k+i|k)$ and $\Delta v(k+i|k)$ denote the predicted manipulated control and the predicted change in manipulated control.

Even better, Adaptive Model Predictive Control (AMPC) can more effectively handle nonlinear systems. AMPC adapts its control parameters in real-time based on changes in system dynamics, making it more responsive to varying conditions compared to standard MPC. This capability allows AMPC to adjust to fluctuations in renewable energy generation or load demands, maintaining stability even when conditions deviate significantly from the expected trajectory. As a modified version of MPC, AMPC enhances the traditional approach by incorporating real-time adaptability, making it particularly well-suited for complex and dynamic environments like microgrids. Its ability to continuously fine-tune the control strategy ensures optimal performance under varying conditions. Figure 2 shows the AMPC block diagram.

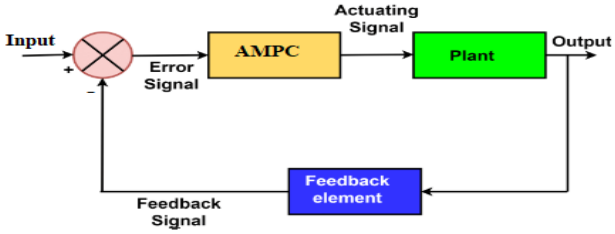

Figure. 2 AMPC block diagram.

This control mechanism, especially for renewable and conventional energy systems, helps in timely adjustment of energy demand and supply. While the OU microgrid operates

International Journal of Scientific Engineering and Science
Volume 8, Issue 12, pp. 40-53, 2024. ISSN (Online): 2456-7361

in grid-connected mode. The existing CHP unit supplies less than 50% of the campus' peak load, which is approximately 9.7 MW. The remaining energy in this research is provided by renewable sources and battery storage, with additional support from the utility grid when needed. The multi-level control architecture makes it possible to control the distribution of energy in real time and the CHP unit minimizes dependence on grid power sources, meanwhile ensuring a constant power supply. The system design and operation are based on the 2023 campus load profile, obtained from Oakland University's facilities management, to enable real-time energy management.

III. Background

- Loads: These are the load consuming energy in the microgrid that may include residential, commercial and industrial loads. This refers to the nature of the energy required to power various items on a university campus, such as buildings, and among other structures which may have diverse energy usage.
- Control systems: These systems control the dynamic functioning of the microgrid, ensuring optimal generation, storage and consumption in the network. They help balance energy flows and provide a fine line between demand and supply of energy. Microgrids can function in two primary operational modes:
- Grid-connected mode: In this mode, the microgrid is connected to the main utility grid to allow bidirectional power flow. During peak demand periods or outages, the grid provides additional support and stability to the microgrid [24].
- Islanding mode: When the main grid experiences a failure or an outage, the microgrid disconnects from the external grid and operates independently. In this scenario, the microgrid continues to supply power to critical loads, ensuring uninterrupted service within its boundaries [25].

A. Multilevel Control Strategy

Microgrids are designed to provide reliable, autonomous, and high-quality power supply.

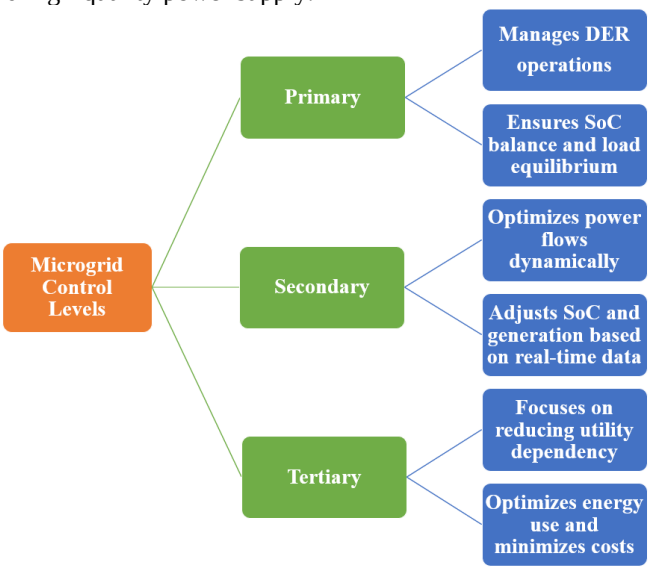

Figure 3. Multi-level diagram for microgrid control

Microgrid control typically involves different levels of control as Figure 3 illustrates, including distribution management systems, central microgrid controllers, and individual source and load controllers [26]. Effective microgrid control is essential for ensuring the stable integration of diverse energy sources, particularly when renewable energy generation fluctuates. In the literature, several control architectures have been developed, each of which has its benefits and drawbacks. control in microgrids typically consists of three levels: primary, secondary, and tertiary control, each with specific responsibilities:

- Primary and Secondary Levels: Responsible for local stability and central operations of the microgrid.
  Tertiary Level: Oversees the interaction between the microgrid and the host network, managing voltage, frequency control, and power balance.

IV. Proposed Methodology

The microgrid, as shown in Figure 4, comprises a utility grid, solar energy, wind turbines, combined heat and power (CHP), and battery storage systems. The system's mathematical model is implemented using MATLAB 2024a.

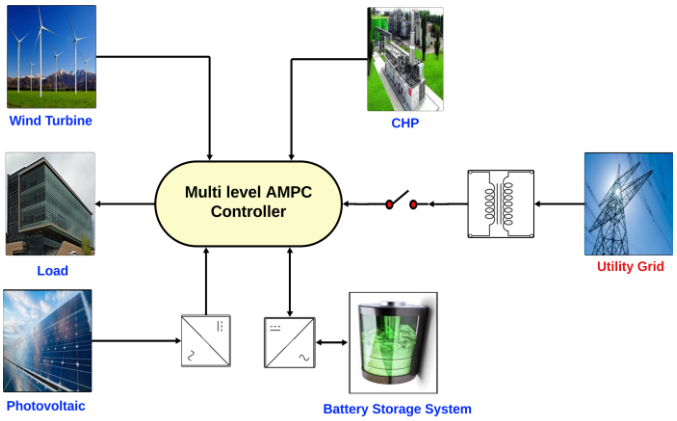

Figure 4. Proposed Microgrid Configuration

Accurate mathematical models of microgrid components are crucial for implementing adaptive Model Predictive Control (AMPC). These models predict system behavior and optimize energy management. The following equations represent key components: solar power generation, wind turbine energy, battery state of charge, and CHP systems. They enable MPC to balance power generation, storage, and consumption while considering system constraints and environmental conditions. This ensures optimal operation, minimal reliance on the external grid, and real-time responsiveness to changing loads and renewable energy availability.

The solar component of the microgrid is modelled based on its efficiency. The power generated by the solar panel in terms of solar irradiation, temperature and efficiency is expressed as [27],[28]:

$$P = G \times A \times \eta \times \left(1 - \beta \times \left(T - T_{ref}\right)\right) \quad (8)$$

Where G is the irradiance, A is the area, η is the efficiency, β is the temperature coefficient, T is the temperature, and T_{ref} is the temperature reference.

International Journal of Scientific Engineering and Science
Volume 8, Issue 12, pp. 40-53, 2024. ISSN (Online): 2456-7361

The energy harnessed from wind increases proportionally to the cube of its speed. So, if wind speed doubles, the turbine's power output increases by a factor of eight. The power from the wind turbine is given by [29], [30]:

$$P_{wind} = 0.5 \times \rho \times A_{turbine} * V_{wind}^3 \times C_p(\lambda, \beta) \times \eta_{turbine} \quad (9)$$

Where: $P_{wind}(t)$, Wind power output at time t (kW) - ρ: Air density (kg/m³) - $A_{turbine}$, Wind turbine rotor swept area (m²) - $V_{wind}(t)$, Wind speed at time t (m/s) - $C_p(\lambda, \beta)$, Power coefficient considering tip-speed ratio (λ) and blade pitch angle (β) (unitless) - $\eta_{turbine}$, Wind turbine efficiency.

The Coulomb counting method, also known as ampere-hour counting or current integration, is the most common approach for estimating the State of Charge (SOC). This technique calculates SOC by integrating the battery's current measurements over its operational period, as shown below [69]:

$$SOC(t+1) = SOC(t) + (\eta_{charge} \times P_{charge}(t) \times \Delta t - P_{discharge}(t) \times \Delta t) / (C_{battery}) \quad (10)$$

Where: - SOC(t): Battery state of charge at time t (%) - η_{charge}: Charging efficiency - $P_{charge}(t)$: Charging power at time t (kW) - $P_{discharge}(t)$: Discharging power at time t (kW) - Δt: Time step (h) - $C_{battery}$: Battery capacity (kWh).

A Combine Heat and Power (CHP), produces both electricity and useful heat from a single fuel source, enhancing overall energy efficiency. The system is modeled by defining load profiles for electrical and thermal demands, which represent the energy needs over time. The electrical output is calculated based on the system's electrical capacity, the fraction of load supplied, and a maximum limit set at half of the electrical capacity. Similarly, the thermal performance is determined by considering the thermal capacity of the system, the delivered load fraction and the ratio of thermal to electrical energy [31]. The equation is given by:

$$chp_{power}(i) = min\left(elec_{cap}, max\left(elec_{load}(i) \times chp_{frac}, 0.5 \times elec_{cap}\right)\right) \quad (11)$$

$$therm_{out}(i) = min\left(\left[therm_{cap}, therm_{load}(i) \times chp_{frac}, \frac{therm_{eff}}{elec_{eff}} \times chp_{power}(i)\right] 2\right) \quad (12)$$

Where chp_{frac} represents the fraction of the load supplied by the CHP system. $elec_{cap}$ and $therm_{cap}$ represent the electrical and thermal capacities of the system, respectively. $elec_{load}$r and $herm_{load}$ present the electrical and thermal loads. $elec_{eff}$ and $therm_{eff}$ represent the efficiencies of the system' electrical and thermal, respectively. chp_{power} represents the electrical output. $therm_{out}$ represents the thermal output.

These formulas ensure that the electrical output and thermal output of the CHP system are within their respective capacity limits while meeting the specified fractions of the load and considering the efficiencies of the system.

Also, the MPC aims to minimize the cost function that considers various factors that simplified as:

$$J = \Sigma \left(cost_{grid} * P_{grid}(t) + cost_{chp} * P_{chp}(t) + cost_{PV}(P_{PV}(t)) + cost_{wind}(P_{wind}(t))\right) \quad (13)$$

Where: - J, Cost function to be minimized - Σ: Summation over the prediction horizon - $cost_{grid}$, Cost of grid power (/kWh)−$P_{grid}(t)$, Grid power at time t (kW) −$cost_{chp}$, Cost of CHP power (/kWh) - P_{chp}, CHP power at time t (kW) - $cost_{PV}(P_{PV}(t))$, Cost of PV power (/kWh).

The adaptive prediction horizon adjustment can be expressed as

$$H_{new} = max\left(H_{min}, min\left(H_{max}, H_{current} + f_{adj} \times \left(P_{renewable}^{pred} - P_{load}^{pred}\right)\right)\right) \quad (14)$$

Where: H_{new}: Adjusted prediction horizon, H_{min}: Minimum allowed prediction horizon, H_{max}: Maximum allowed prediction horizon, $H_{current}$: Current prediction horizon, f_{adj}: Adjustment factor (scaling factor for horizon adjustment), $P_{renewable}^{pred}$: Predicted total renewable power (kW), P_{load}^{pred}: Predicted load (kW).

This equation demonstrates how the prediction horizon can be dynamically adapted to optimize the performance of AMPC system within the microgrid. The prediction horizon refers to the time period over which AMPC forecasts future system behavior and makes control decisions. By adjusting this horizon in real time based on predicted renewable energy generation and load demand, the system can efficiently manage energy resources.

When the predicted renewable power ($P_{renewable}^{pred}$) exceeds the predicted load (P_{load}^{pred}), the system extends the prediction horizon. This extension allows for a longer-term view, enabling the AMPC to make decisions that account for surplus energy, such as charging the Battery Storage System (BSS) or reducing grid power consumption. In contrast, when renewable power and load are closely matched, a shorter prediction horizon helps the system respond quickly without overburdening computational resources. The adjustment factor (f_{adj}) regulates how much the prediction horizon changes based on the difference between renewable power and load. The equation ensures that the horizon stays within practical limits, defined by (H_{min}) and (H_{man}), keeping the system efficient and adaptable.

Figure 5 shows the control strategy for the grid-connected microgrid, detailing multi-level decision-making with AMPC for real-time adjustments. The hierarchical system efficiently balances energy generation and consumption, reducing grid reliance and optimizing performance.

The system checks if power from photovoltaics (PV), wind turbines (WT), and combined heat and power (CHP) systems meets the load demand. If demand exceeds generation, the Battery Storage System (BSS) fills the gap. If both renewable sources and the BSS are insufficient, the CHP adjusts output, with grid power as a last resort. Excess PV and WT power charges the BSS, maximizing renewable use and minimizing grid reliance.

AMPC forecasts load demands and adjusts power flows in real time, optimizing performance and synchronizing control layers. The primary level manages Distributed Energy Resources (DERs) and storage, processes local data, and communicates with the secondary level. The secondary level oversees multiple DERs, processes data, and uses AMPC to set

control points, while the tertiary level coordinates the entire microgrid, setting objectives for the secondary level.

A key component of the secondary control is a controller [32], that uses a cost function to minimize power tracking errors, optimize fuel use, and reduce battery wear. It operates within DER and storage limits to ensure safe battery performance. AMPC leverages real-time data to forecast system behavior and adjust actions, promoting efficient, stable microgrid operation, reducing grid dependence, and lowering costs.

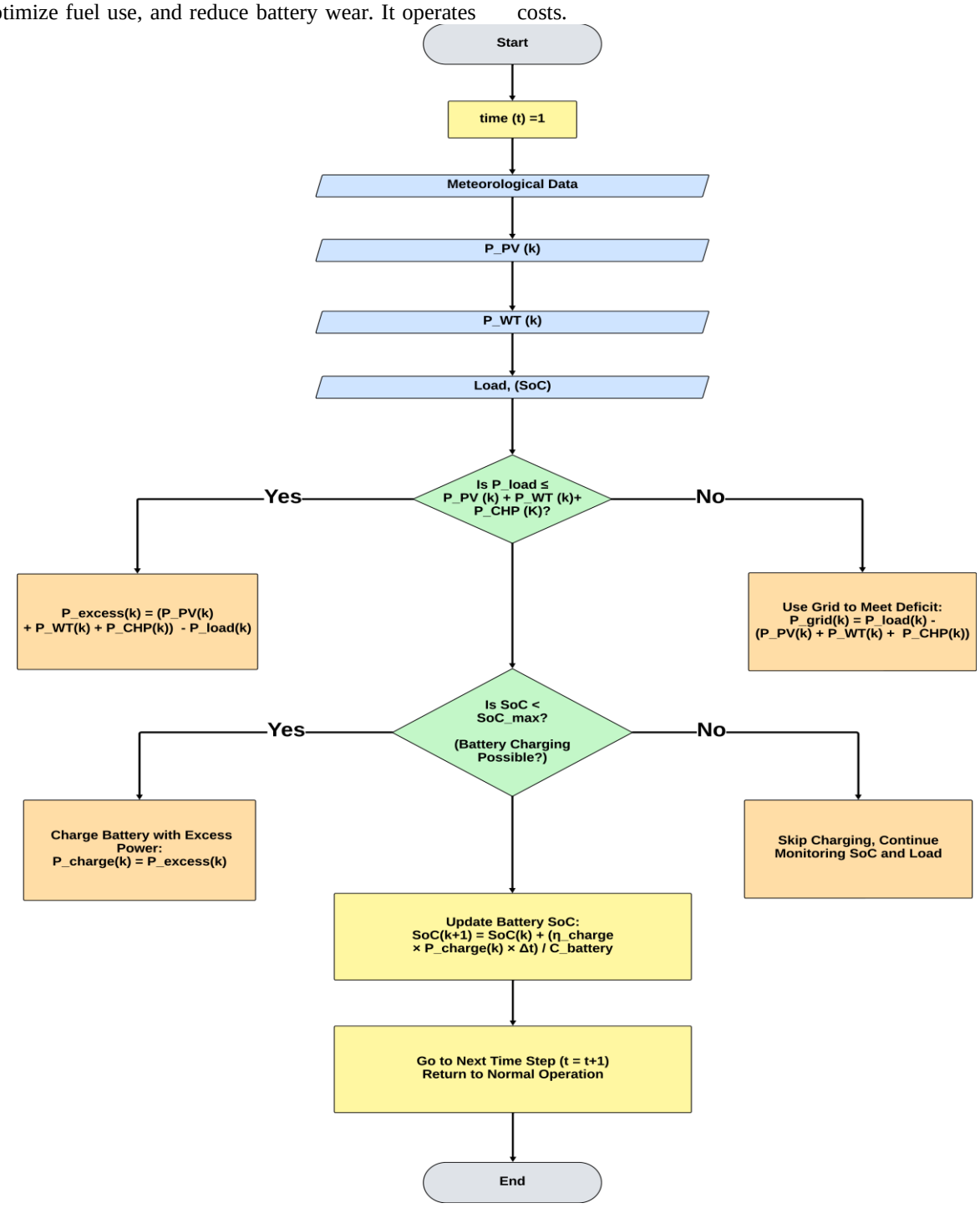

Figure 5. Microgrid Multi-levels Control Flowchart

V. Simulation and Results

The Simulations used data from NREL and Oakland University's 2023 load profile. Key peak load dates were selected to assess the controller's adaptability.

- Meteorological and Load Data Visualization

This This section presents visualizations of meteorological data, including solar irradiance, wind speed, and temperature, alongside load demand data. These visuals highlight the interaction between environmental conditions and energy

International Journal of Scientific Engineering and Science
Volume 8, Issue 12, pp. 40-53, 2024. ISSN (Online): 2456-7361

consumption, demonstrating how weather and seasonal changes affect system performance.

Figure 6 shows that winter irradiance, slightly over 200 W/m², reduces solar panel output to 0W due to freezing temperatures. The average wind speed of 5 m/s is optimal for wind turbines, while the electrical load peaks at 5,500 kW around midday.

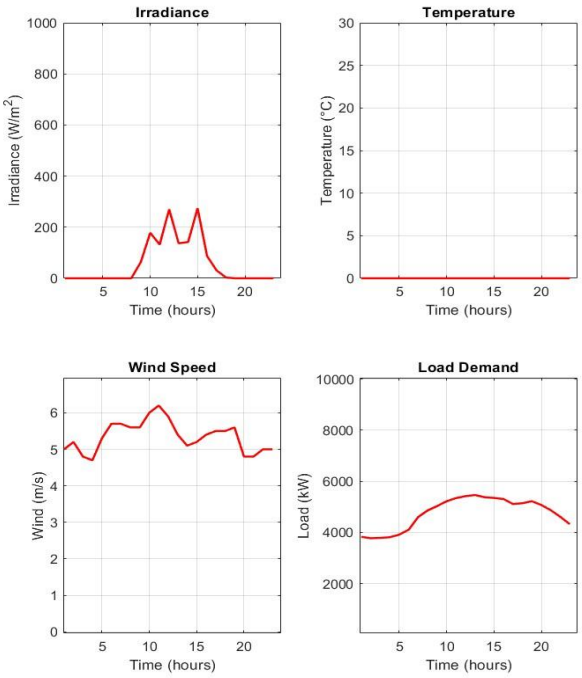

Figure 6. Winter Daily Meteorological and Load data

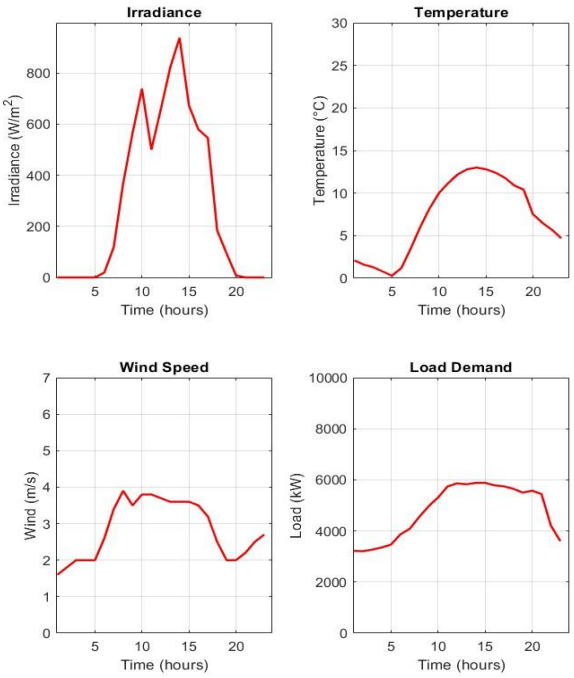

Figure 7. Spring Daily Meteorological and Load Demand

Figure 7 shows that during the spring season, sunlight intensity exceeds 800 W/m², boosting solar power output, while relatively low temperatures support efficient PV operation. However, inadequate wind reduces wind energy generation. The load varies, peaking around 6,000 kW midday. The system's primary control manages power flow and generation, ensuring continuous feedback.

Figure 8 shows summer irradiance over 800 W/m², generating solar power, with midday temperatures around 25°C. Wind energy is minimal due to 2 m/s winds. Power peaks at 7,000 kW, driven by cooling systems, with primary and secondary controls managing energy supply and storage.

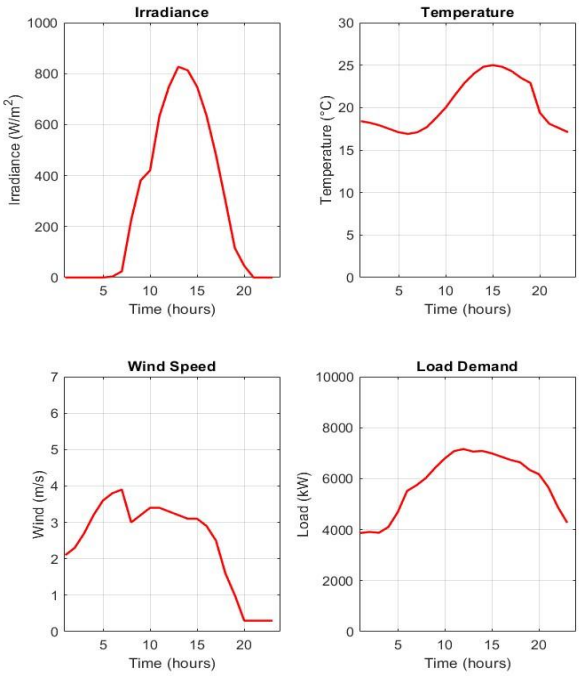

Figure 8. Summer Daily Meteorological and Load Demand

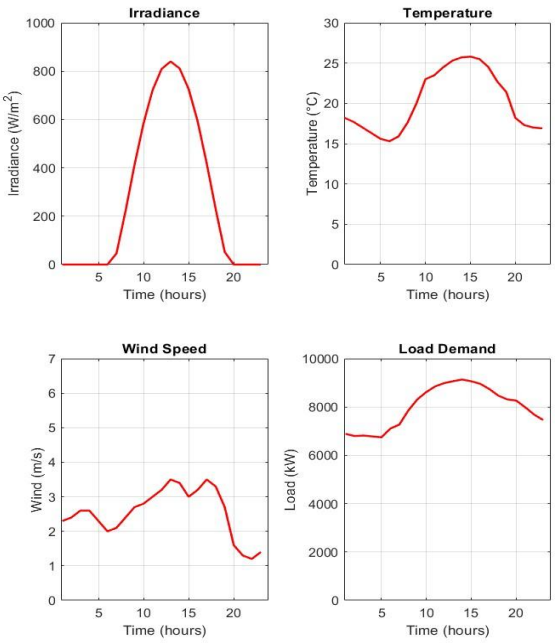

Figure 9. Fall Daily Meteorological and Load Demand

Figure 9 shows that the fall season has favorable conditions with irradiance over 800 W/m² and temperatures around 26°C in the late afternoon. Wind speeds average 2.5 m/s, contributing moderately to energy generation. The load exceeds 9,000 kW due to full attendance. Key controls manage data, generation, and demand.

A. *Seasonal Power Output Comparisons*

The power output profiles across seasons are illustrated in Figures 10 through 14, showcasing the output from solar, wind, and CHP systems during winter, spring, summer, and fall, respectively. These figures are in correlation with the first control level of the adaptive multi-level control scheme as the subsequent control action is obtained after gathering data from DERs in real time.

Figure 10 shows no solar power output during winter due to low irradiation or snow-covered panels. Wind power fluctuates with varying wind speeds, while CHP provides stable output, compensating for the unreliable solar generation.

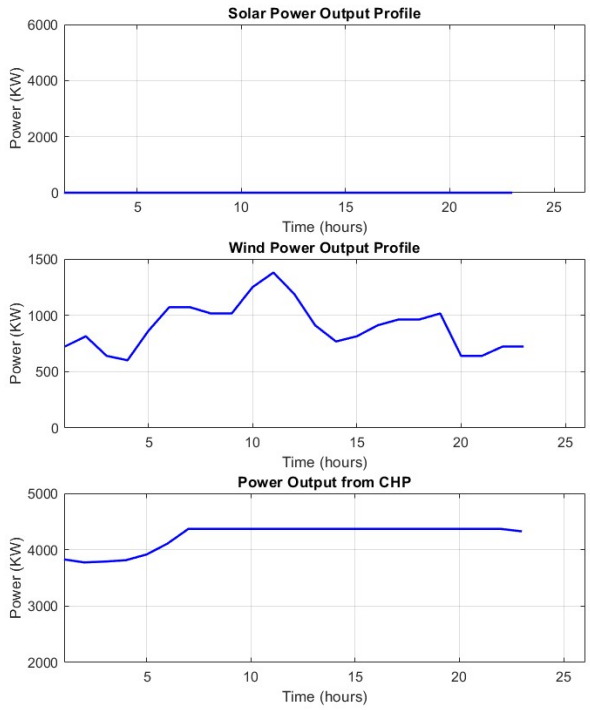

Figure 10. Winter Power Output: Solar, Wind, and CHP

Figure 11 shows a mid-day peak in solar power output, typical of better spring irradiation. Wind power remains stable, while CHP output slightly declines later in the day but continues to provide reliable support to meet demand.

Figure 12 shows solar power peaking at midday due to strong summer irradiation, providing significant energy. Wind power remains mostly constant with a slight decrease, likely due to lower wind speeds. CHP output starts low in the morning but quickly stabilizes, reliably meeting base load requirements throughout the day.

Figure 13 shows a significant solar power peak during the day, lower than summer levels but still substantial due to shorter days and lower sun altitude in fall. Wind power remains stable with minor fluctuations, indicating moderate wind conditions. CHP output is constant throughout the day, reliably meeting the base load demand.

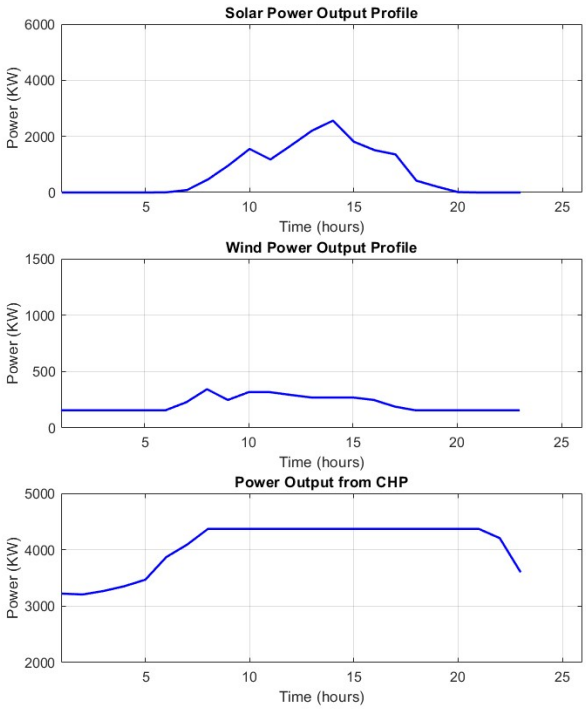

Figure 11. Spring Power Output: Solar, Wind, and CHP

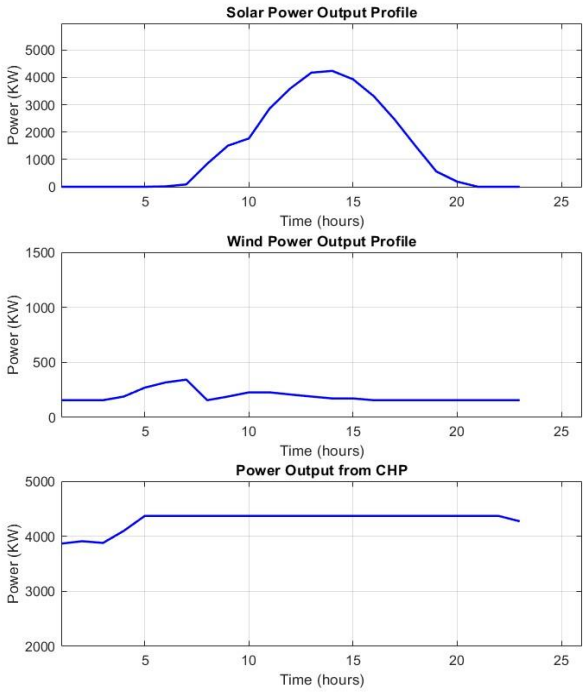

Figure 12. Summer Power Output: Solar, Wind, and CHP

B. *Microgrid Dynamics: Results*

Microgrids continuously adjust power production in real time, responding to fluctuations in renewable energy and battery charge by recalibrating outputs based on current generation and demand. Results from MPC and modified AMPC will be compared to highlight differences in managing renewable energy and storage.

International Journal of Scientific Engineering and Science
Volume 8, Issue 12, pp. 40-53, 2024. ISSN (Online): 2456-7361

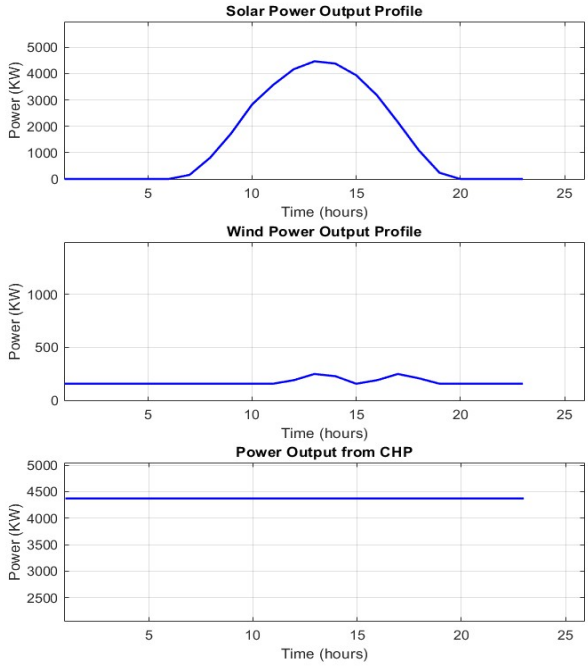

Figure 13. Fall Power Output: Solar, Wind, and CHP

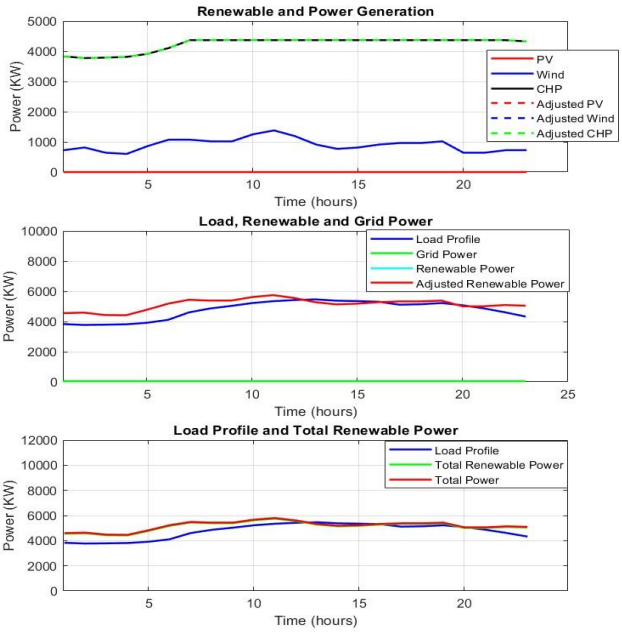

Figure 14. Load Profiles: Renewable vs. Grid Power in Winter

1. MPC Results

- Winter power generation

The analysis shows no solar power during winter, significantly impacting energy supply. Wind turbines (WT) and CHP systems provide power, but their combined output is insufficient to meet demand, as shown in Figure 14. The grid supplies no power, revealing a critical gap in energy management.

Figure 15 shows ESS performance in spring. Excess power charges the battery fully, but the controller fails to discharge it to meet demand, revealing inefficiency in the control strategy.

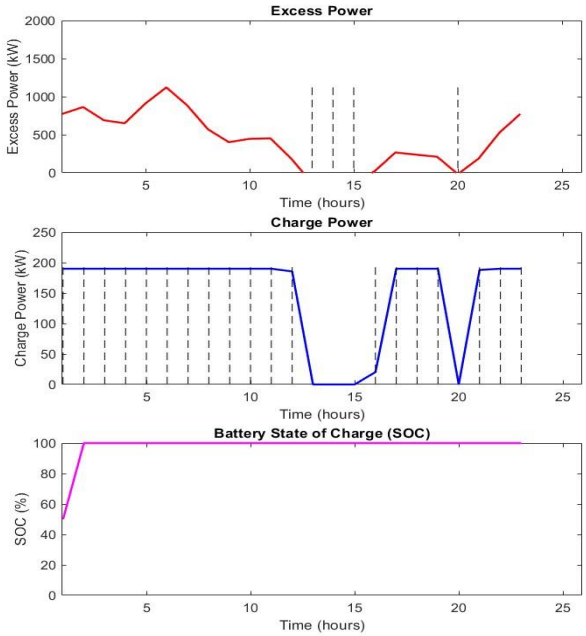

Figure 15 Winter Excess Power, Charging, and Battery SOC

- Spring power generation

Figure 16 shows minimal wind turbine power in spring, while solar generation rises from 7 AM to 7 PM and decreases in the evening. Despite strong solar output, the load demand is still unmet, indicating a supply deficit.

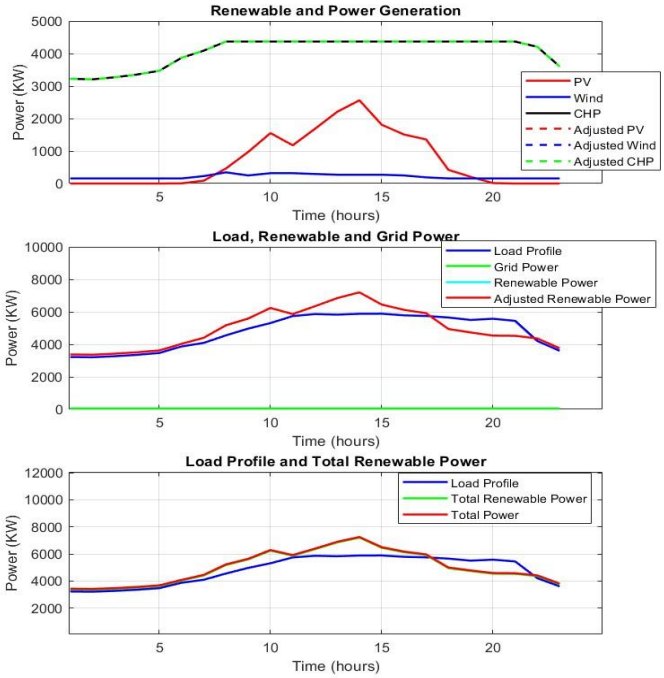

Figure 16 Load Profiles: Renewable vs. Grid Power in Spring

Figure 17 shows ESS performance in spring, with excess power charging the battery to full capacity. However, the controller fails to discharge the ESS when needed, missing the

International Journal of Scientific Engineering and Science
Volume 8, Issue 12, pp. 40-53, 2024. ISSN (Online): 2456-7361

opportunity to meet demand. This highlights a limitation in the control strategy, as stored energy is not used to address load deficits.

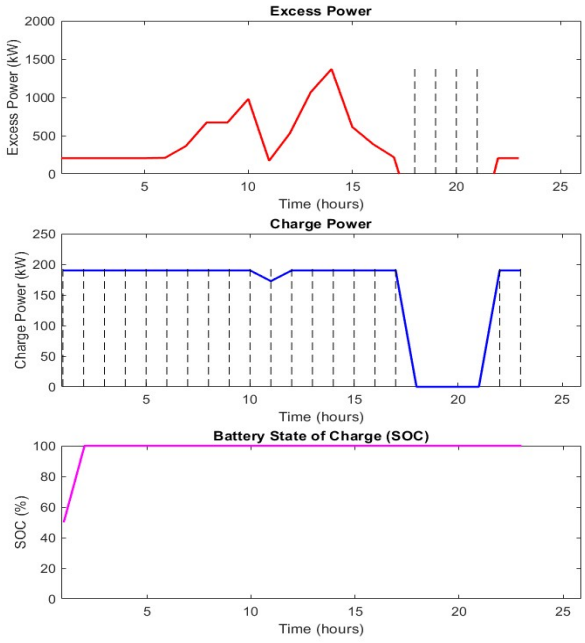

Figure 17 Spring Excess Power, Charging, and Battery SOC

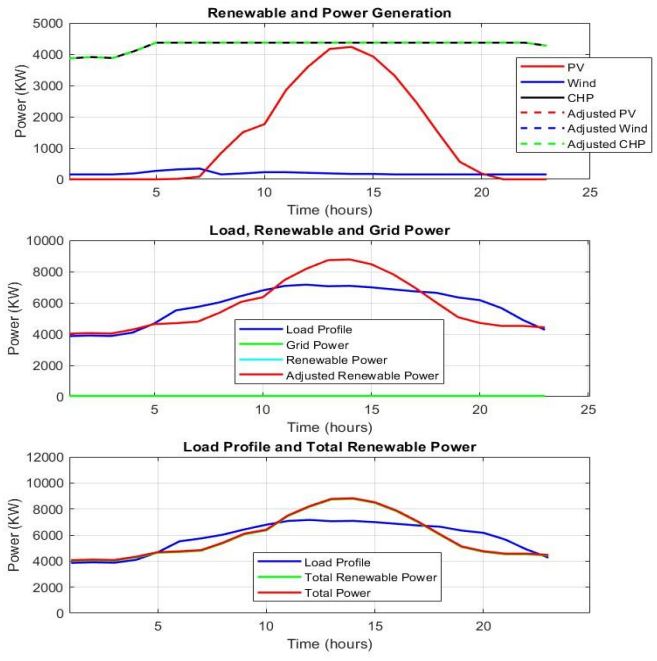

Figure 18 Load Profiles: Renewable vs. Grid Power in Summer

- Summer power generation

Figure 18 shows summer energy dynamics, with high load demand primarily supported by CHP and solar power, and minimal wind turbine contribution. CHP and WT meet early morning demand, while solar supports the load from 7 AM to 8 PM. However, power deficits occur between 5 AM and 10 AM, and from 7 PM to midnight. The grid is not utilized, leading to unmet load demand during these critical periods due to controller weakness.

Figure 19 shows that despite significant excess power during summer, the ESS remains underutilized. The controller fails to discharge the battery to meet demand, leaving the SOC at full capacity. This inefficiency highlights a key flaw in the control strategy, as stored energy is not used to address demand peaks.

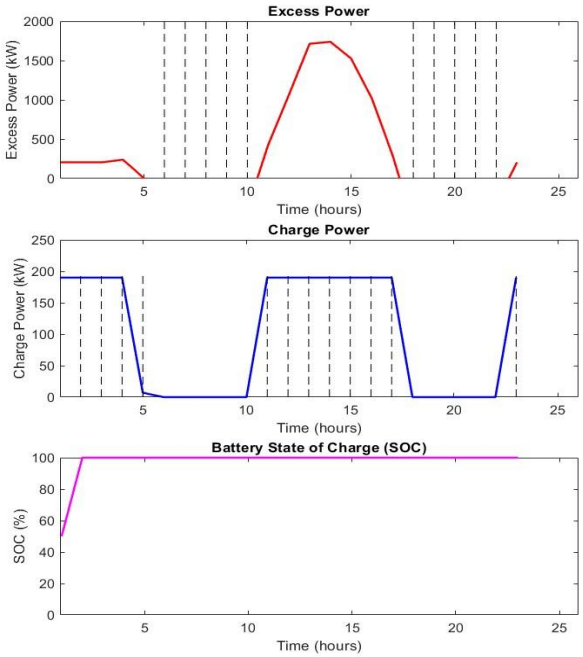

Figure 19 Summer Excess Power, Charging, and Battery SOC

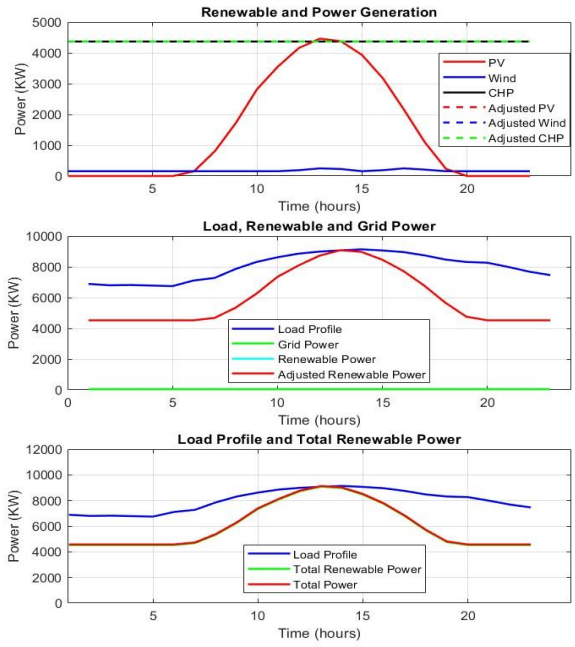

Figure 20 Load Profiles: Renewable vs. Grid Power in Fall

- Fall power generation

International Journal of Scientific Engineering and Science
Volume 8, Issue 12, pp. 40-53, 2024. ISSN (Online): 2456-7361

Figure 20 shows that in the fall season, solar power peaks during daylight hours, while wind generation remains minimal. The fluctuating load often exceeds renewable generation, and the grid is not used effectively to cover these deficits.

Figure 21 reveals critical ESS performance issues during summer, with no excess power generated and only a brief charging event. The battery SOC remains stable but underutilized, showing the control strategy's failure to effectively manage energy resources and meet fluctuating load demands.

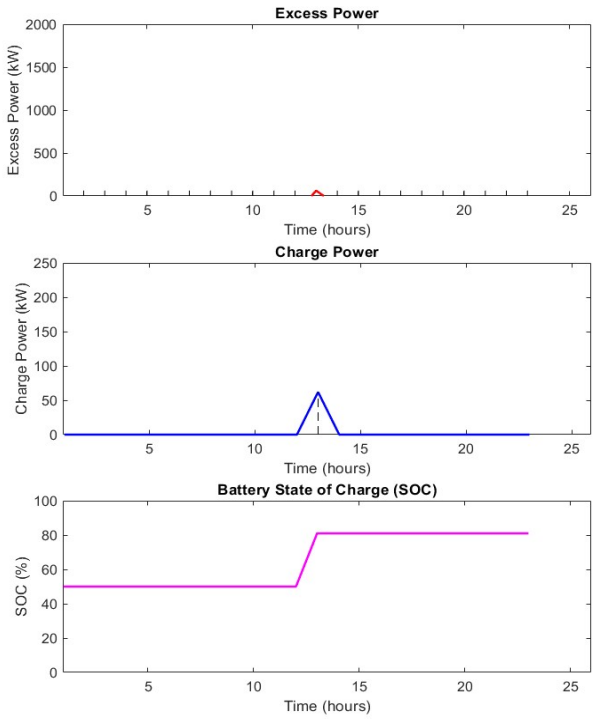

Figure 21 Fall Excess Power, Charging, and Battery SOC

1. AMPC Results

- Winter power generation

Figure 22 shows the operational dynamics on a winter day, highlighting the integration of solar, wind, CHP, and grid power in primary control. Real-time data balances load demands between renewable and grid sources, while the adaptive MPC system optimizes energy allocation to reduce grid dependence and improve efficiency.

Figure 23 illustrates the management of excess power, battery charging, and SOC adjustments. The system efficiently handles battery usage to maintain stability, using surplus wind power during the day for charging. In winter, with no solar energy, excess power mainly comes from wind. At night, reduced consumption generates surplus power, which the system strategically manages by charging batteries during the day for nighttime use. The alternating charge and discharge cycles, shown in the graph, are key to maintaining system stability.

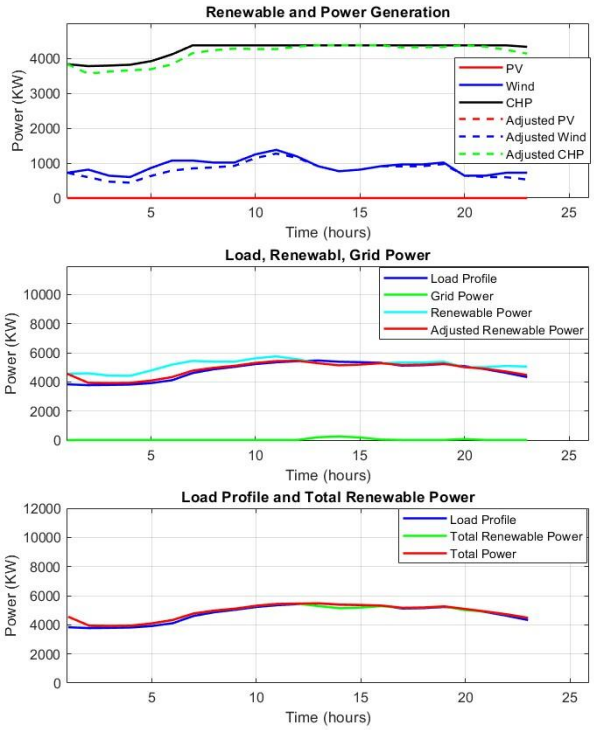

Figure 23. Load Profiles: Renewable vs. Grid Power in Winter

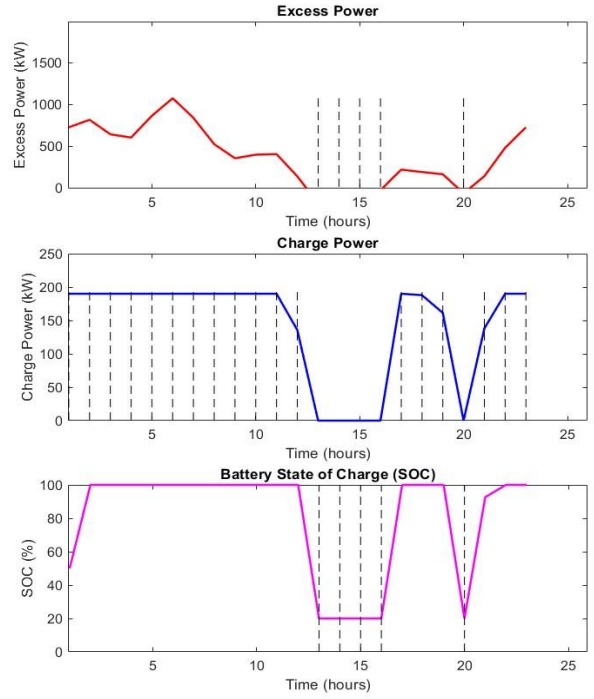

Figure 23. Winter Excess Power, Charging, and Battery SOC

- Spring power generation

In spring, there is a slight increase in solar energy generation, which reduces grid dependence, as in Figure 22. The secondary control mechanisms maintain a balance between

generated and grid-supplied power, optimizing efficiency without exceeding generation capacity limits.

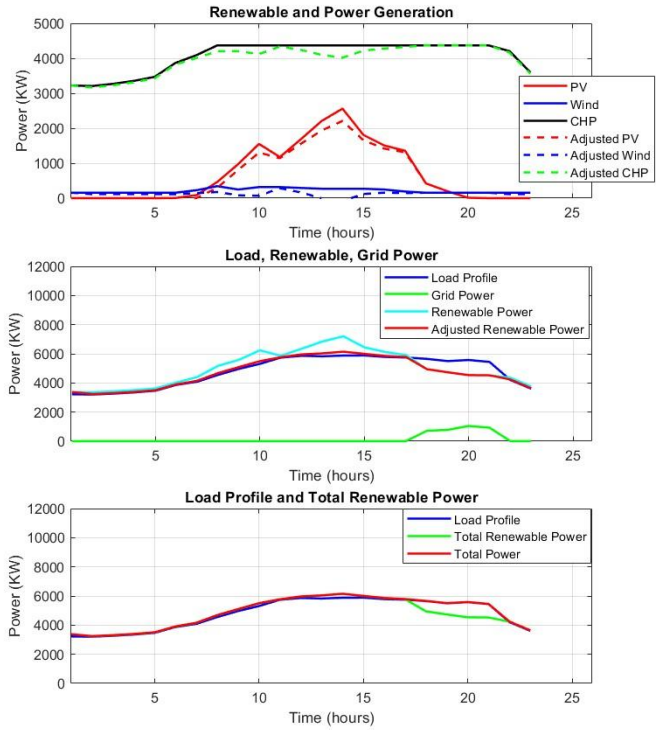

Figure 22. Load Profiles: Renewable vs. Grid Power in Spring

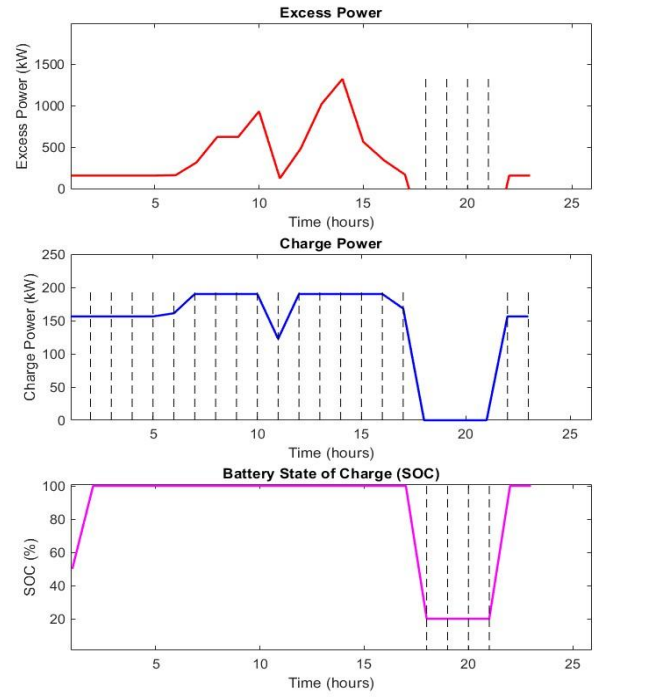

Figure 23. Spring Excess Power, Charging, and Battery SOC

Figure 23 highlights battery management in spring, showing midday excess power from solar charging the batteries, as wind contributions remain low. The battery SOC rises significantly, prioritizing solar energy for charging. At night, batteries supply power to meet demand, ensuring reliable energy and reducing grid dependency.

- Summer power generation

As depicted in Figure 24, during the summer months, solar power generation reaches its peak, significantly reducing reliance on grid power, particularly during daylight hours. The tertiary control system demonstrates a high level of autonomy by effectively managing surplus energy, either by storing it or directing it to non-critical loads, optimizing overall system efficiency.

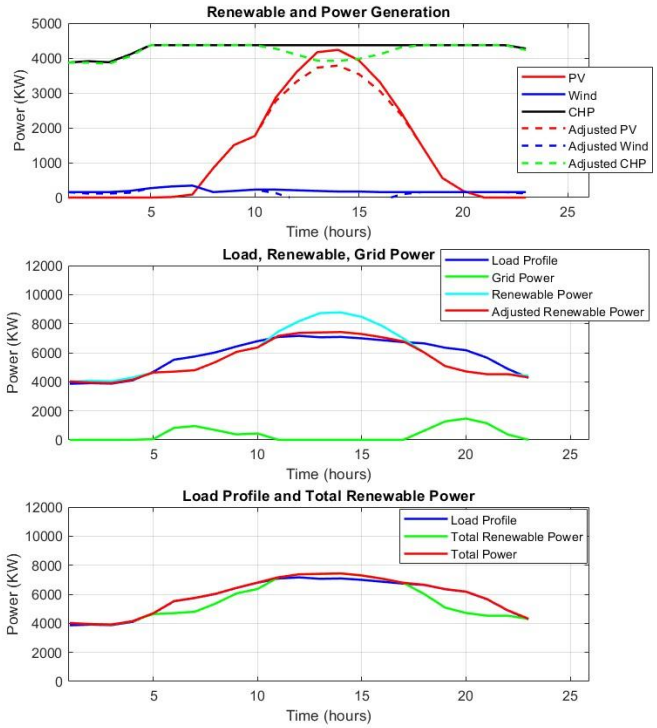

Figure 24. Load Profiles: Renewable vs. Grid Power in Summer

Figure 25 shows the summer energy management system relying on solar power due to low wind speeds. The battery supplies power from 5 AM to 10 AM, charges during peak solar hours, and discharges again from 4 PM to 11 PM. Excess solar power charges the battery, and the SOC graph reflects stable energy management, maintaining system stability after peak charging.

- Fall power generation

Figure 26 shows fall as a transitional phase with increased reliance on grid power due to fluctuating solar and wind generation. Adaptive control systems efficiently manage grid power, ensuring a stable energy supply as renewable sources become more intermittent, demonstrating the system's adaptability.

Figure 27 shows renewable energy generation and power management within the microgrid over a specific period. It highlights efficient operation of photovoltaic (PV) panels and the CHP system during peak hours. However, at times, the load exceeds available solar power, leaving no excess energy to charge the battery.

International Journal of Scientific Engineering and Science
Volume 8, Issue 12, pp. 40-53, 2024. ISSN (Online): 2456-7361

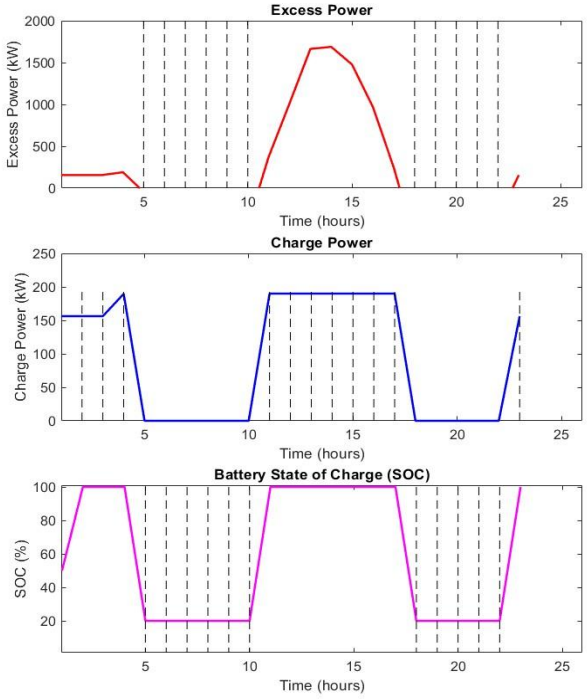

Figure 25. Summer Excess Power, Charging, and Battery SOC

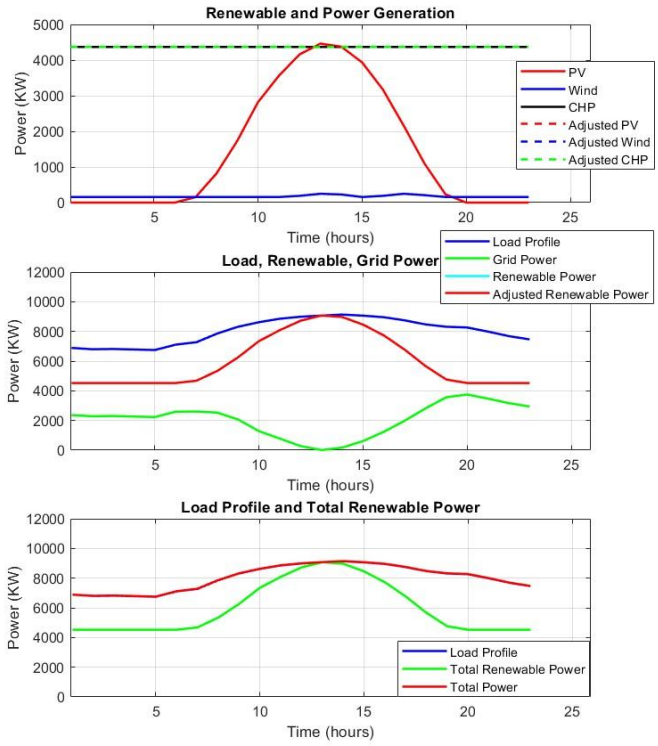

Figure 26. Load Profiles: Renewable vs. Grid Power in Fall

- AMPC vs. Basic MPC Performance

The results obtained from the analysis of basic MPC and Adaptive MPC indicate that AMPC outperforms basic MPC in effectively meeting load demand from various energy sources. Throughout the day, AMPC demonstrates superior capability in discharging ESS to supply power when needed. Additionally, it efficiently calls on utility support during periods of insufficient renewable generation. This adaptability ensures a more reliable energy management process, ultimately enhancing the overall performance of the microgrid.

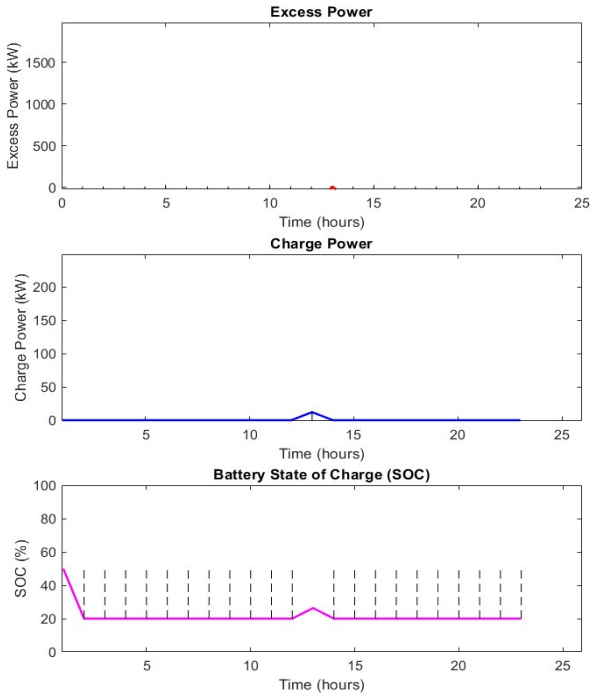

Figure 27. Fall Excess Power, Charging, and Battery SOC

C. AMPC for Seasonal Energy Management

During winter, solar energy is nearly absent, relying mainly on wind power and grid support. Battery storage ensures a reliable energy supply during peak demand, even when wind is insufficient. In spring, improved sunlight reduces grid usage, and excess solar energy charges the batteries for use during low solar output.

In summer, solar power meets the load demand, with surplus energy charging the batteries, allowing the microgrid to operate almost entirely on renewables without grid reliance. Fall sees good solar generation, with solar and wind energy combined with battery storage to meet energy needs. The system effectively transitions from solar to wind in the evening, maintaining a stable power output using stored energy.

This year-round battery management approach addresses seasonal renewable energy variability, reducing grid reliance during high renewable output in spring and summer, and compensating for lower outputs in fall and winter. Adaptive control systems effectively manage fluctuations in energy production and consumption, ensuring system stability and optimal performance.

D. Seasonal Cost Analysis

- Grid Energy Costs Without Microgrid

International Journal of Scientific Engineering and Science
Volume 8, Issue 12, pp. 40-53, 2024. ISSN (Online): 2456-7361

Energy price varies considerably by season and the fall season reaches a top of $21,600, which is attributed to higher consumption or more expensive utility costs. Among seasons, spring has the lowest at $13,824. Cost figures for costs associated with winter and spring are almost the same, with winter costs at $14,544 and summer rising to $15,840, because of refrigerator and air conditioning loads. These changes are displayed in Figure 28, while also indicating the volatility of grid-related costs.

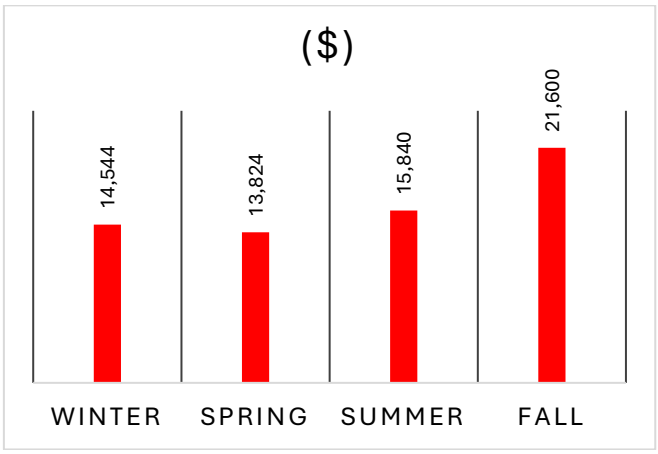

Figure 28. Grid Energy Without Microgrid

- Seasonal Costs with Microgrid

Microgrid implementation balances energy costs across seasons, with winter and fall nearing $11,000 due to higher demand, while spring and summer are lower, around $9,000, benefiting from solar efficiency. Figure 39 highlights this trend, showing stable costs despite varying seasonal demands. The microgrid effectively manages energy consumption throughout the day.

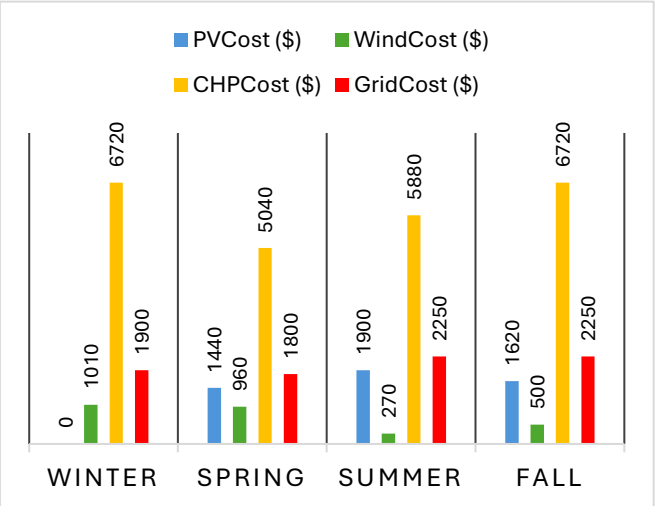

Figure 29. Post-Microgrid Seasonal Costs

- Total Microgrid Energy Costs Per Season

The microgrid ensures a balanced distribution of energy costs across seasons. Winter and fall relate to the highest cost of $11,000. Spring and summer are lower, with spring being the least expensive at just over $9,000. Figure 30 illustrates this stability, highlighting the microgrid's ability to manage seasonal variations effectively. This approach ensures that there are no fluctuations in energy costs during the time of the day.

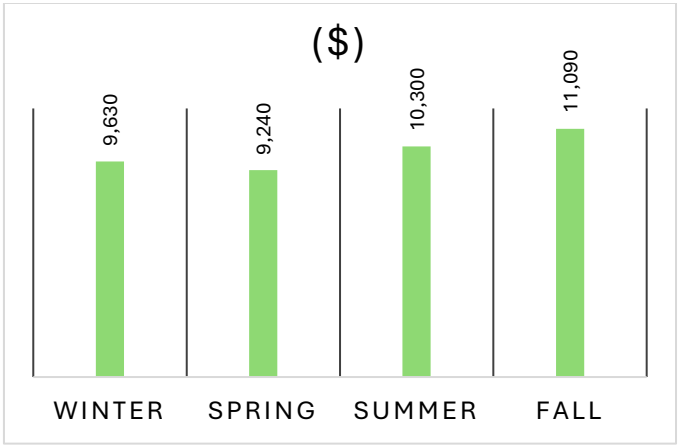

Figure 30. Total Seasonal Energy Cost with Microgrid

- Seasonal Cost Savings with Microgrid

The microgrid provides significant energy cost savings, varying across seasons. Fall achieves the highest savings, exceeding $10,000, due to reduced reliance on traditional grid power. Winter, spring, and summer see more moderate savings, around $4,000 to $6,000. Figure 31 highlights these seasonal savings, showcasing the microgrid's ability to align energy generation with demand. This trend demonstrates its potential to reduce costs throughout the year.

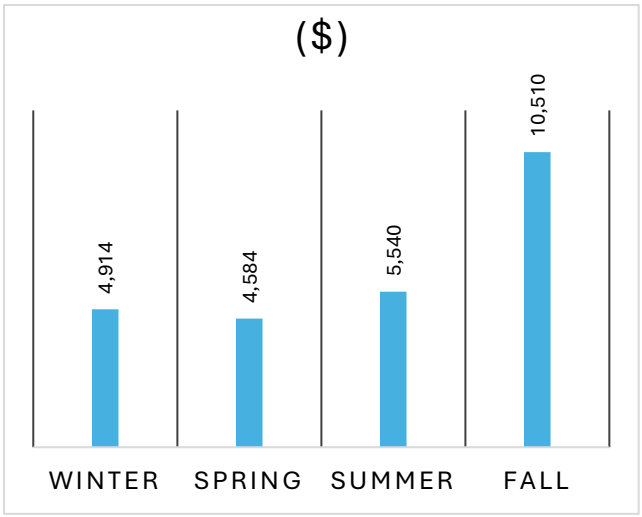

Figure 31 Seasonal Savings

VI. Conclusion

This research presented an advanced multi-level control system using Adaptive Model Predictive Control (AMPC) to manage a grid-connected microgrid, with Oakland University as the case study. The system operated across three hierarchical levels: at the primary level, it regulated Distributed Energy Resources (DERs) such as PV, wind turbines, and CHP systems to ensure a real-time balance between power generation and

demand. The secondary level dynamically optimized energy distribution, adjusting power flows based on real-time conditions to reduce grid dependence. The tertiary level focused on long-term energy management, aiming to minimize reliance on external power and maximize renewable energy use.

The comparative analysis of basic and adaptive control strategies revealed that the adaptive approach outperformed the traditional method in managing load demand from diverse energy sources. Throughout the day, the system exhibited superior performance in discharging ESS when needed and leveraged utility support during periods of insufficient renewable generation. This adaptability ensured a more reliable and efficient energy management process for the microgrid.

Through the tertiary level, the microgrid delivered significant seasonal cost savings. Fall achieved the highest daily savings, exceeding $10,000, due to reduced grid reliance, while winter, spring, and summer recorded more moderate savings of $4,000 to $6,000 per day. Seasonal simulations confirmed that the system-maintained power quality, reduced costs, and efficiently managed energy. These results demonstrated the effectiveness of the proposed control system in achieving a balanced, efficient, and sustainable energy management solution for the microgrid.

REFERENCES

[1] K. Salhein, C. Kobus, and M. Zohdy, "Forecasting installation capacity for the top 10 countries utilizing geothermal energy by 2030," *Thermo,* vol. 2, no. 4, pp. 334-351, 2022.
[2] K. Salhein, J. Ashraf, and M. Zohdy, "Output temperature predictions of the geothermal heat pump system using an improved grey prediction model," *Energies,* vol. 14, no. 16, p. 5075, 2021.
[3] K. Salhein, C. Kobus, M. Zohdy, A. M. Annekaa, E. Y. Alhawsawi, and S. A. Salheen, "Heat Transfer Performance Factors in a Vertical Ground Heat Exchanger for a Geothermal Heat Pump System," *Energies,* vol. 17, no. 19, p. 5003, 2024.
[4] M. Hawsawi, H. M. D. Habbi, E. Alhawsawi, M. Yahya, and M. A. Zohdy, "Conventional and Switched Capacitor Boost Converters for Solar PV Integration: Dynamic MPPT Enhancement and Performance Evaluation," *Designs,* vol. 7, no. 5, p. 114, 2023.
[5] A. Barnawi, M. A. Zohdy, and T. Hawsawi, "Determining the Factors Affecting Solar Energy Utilization in Saudi Housing: A Case Study in Makkah," *Energies,* vol. 16, no. 20, p. 7196, 2023.
[6] E. Y. Alhawsawi, K. Salhein, and M. A. Zohdy, "A Comprehensive Review of Existing and Pending University Campus Microgrids," *Energies,* vol. 17, no. 10, p. 2425, 2024.
[7] M. Kiehbadroudinezhad *et al.*, "The role of energy security and resilience in the sustainability of green microgrids: Paving the way to sustainable and clean production," *Sustainable Energy Technologies and Assessments,* vol. 60, p. 103485, December 2023.
[8] E. Y. Alhawsawi, H. M. D. Habbi, M. Hawsawi, and M. A. Zohdy, "Optimal design and operation of hybrid renewable energy systems for Oakland university," *Energies,* vol. 16, no. 15, p. 5830, 2023.
[9] A. Hussain, V.-H. Bui, and H.-M. Kim, "Microgrids as a resilience resource and strategies used by microgrids for enhancing resilience," *Applied Energy,* vol. 240, pp. 56–72, April 2019.
[10] Y. E. García Vera, R. Dufo-López, and J. L. Bernal-Agustín, "Energy Management in Microgrids with Renewable Energy Sources: A Literature Review," *Applied Sciences,* vol. 9, p. 3854, September 2019.
[11] J. A. P. Lopes, A. G. Madureira, and C. Moreira, "A View of Microgrids," in *A View of Microgrids*, ed: Wiley, 2019, pp. 149–166.
[12] M. Abusaq and M. A. Zohdy, "Optimal Sizing of Solar Off Grid Microgrid Using Modified Firefly Algorithm."
[13] K. Salhein, C. Kobus, and M. Zohdy, "Control of heat transfer in a vertical ground heat exchanger for a geothermal heat pump system," *Energies,* vol. 15, no. 14, p. 5300, 2022.
[14] K. A. A. Salhein, *Modeling and Control of Heat Transfer in a Single Vertical Ground Heat Exchanger for a Geothermal Heat Pump System*. Oakland University, 2023.
[15] K. Salhein, C. Kobus, and M. Zohdy, "Heat Transfer Control Mechanism in a Vertical Ground Heat Exchanger: A Novel Approach," 2023.
[16] F. Yakub and Y. Mori, "Model predictive control for car vehicle dynamics system-comparative study," in *2013 IEEE Third International Conference on Information Science and Technology (ICIST)*, 2013: IEEE, pp. 172-177.
[17] A. Khodayari, A. Ghaffari, M. Nouri, S. Salehinia, and F. Alimardani, "Model Predictive Control system design for car-following behavior in real traffic flow," in *2012 IEEE International Conference on Vehicular Electronics and Safety (ICVES 2012)*, 2012: IEEE, pp. 87-92.
[18] L.-h. Luo, H. Liu, P. Li, and H. Wang, "Model predictive control for adaptive cruise control with multi-objectives: comfort, fuel-economy, safety and car-following," *Journal of Zhejiang University SCIENCE A,* vol. 11, no. 3, pp. 191-201, 2010.
[19] H. Yan, M. A. Zohdy, E. Alhawsawi, and A. Mahmoud, "Trajectory State Model-based Reinforcement Learning for Truck-trailer Reverse Driving," in *2024 8th International Conference on Robotics, Control and Automation (ICRCA)*, 2024: IEEE, pp. 197-205.
[20] D. Kestering, S. Agbleze, H. Bispo, and F. V. Lima, "Model predictive control of power plant cycling using Industry 4.0 infrastructure," *Digital Chemical Engineering,* vol. 7, p. 100090, 2023.
[21] D. Kenefake *et al.*, "A smart manufacturing strategy for multiparametric model predictive control in air separation systems," *Journal of Advanced Manufacturing and Processing,* vol. 4, no. 4, p. e10120, 2022.
[22] A. Tyagounov, "High-performance model predictive control for process industry," 2004.
[23] X. Yang, G. Liu, A. Li, and V. D. Le, "A predictive power control strategy for DFIGs based on a wind energy converter system," *Energies,* vol. 10, no. 8, p. 1098, 2017.
[24] G. Shahgholian, "A brief review on microgrids: Operation, applications, modeling, and control," *International Transactions on Electrical Energy Systems,* vol. 31, March 2021.
[25] A. C. Z. de Souza, B. De Nadai N., F. M. Portelinha, D. Marujo, and D. Q. Oliveira, "Microgrids Operation in Islanded Mode," in *Sustainable Development in Energy Systems*: Springer International Publishing, 2017, pp. 193–215.
[26] M. Yazdanian and A. Mehrizi-Sani, "Distributed control techniques in microgrids," *IEEE transactions on smart grid,* vol. 5, no. 6, pp. 2901-2909, 2014.
[27] S. Dubey, J. N. Sarvaiya, and B. Seshadri, "Temperature Dependent Photovoltaic (PV) Efficiency and Its Effect on PV Production in the World – A Review," *Energy Procedia,* vol. 33, pp. 311–321, 2013.
[28] L. S. Pantic, T. M. Pavlović, D. D. Milosavljević, I. S. Radonjic, M. K. Radovic, and G. Sazhko, "The assessment of different models to predict solar module temperature, output power and efficiency for Nis, Serbia," *Energy,* vol. 109, pp. 38–48, August 2016.
[29] L. M. Fernández, C. A. García, and F. Jurado, "Modelling and Control of Wind Turbines," in *Energy Systems*: Springer Berlin Heidelberg, 2013, pp. 443–508.
[30] G. Modukpe and D. Dei, "Modeling and Simulation of a 10 kW Wind Energy in the Coastal Area of Southern Nigeria: Case of Ogoja," in *Wind Solar Hybrid Renewable Energy System*: IntechOpen, 2020.
[31] EPA, "Methods for calculating CHP efficiency," ed: Environmental Protection Agency, 2020.
[32] M. Schwenzer, M. Ay, T. Bergs, and D. Abel, "Review on model predictive control: An engineering perspective," *The International Journal of Advanced Manufacturing Technology,* vol. 117, no. 5, pp. 1327-1349, 2021.